

shallow optical potential emphasizes the core-exchange effect too much.¹² It is also found that the contribution from the nonorthogonality term $[\epsilon - (T + U)]K^{(1)}$ is negligibly small.⁷ The cross sections calculated without the nonorthogonality term are very close to those with the full kernel (the solid line in Fig. 2). This result is consistent with the fact that the multistep-exchange effect is very small, since the nonorthogonality term does not play any role in the first-order perturbation treatment.⁷

In conclusion, for $^{16}\text{O} + ^{18}\text{O}$ scattering, core-exchange model analyses with the full-recoil effect give a consistent interpretation of the observed incident-energy dependence of the backward cross sections. The multistep core-exchange effect has not been found to be important in the present analyses nor has the effect due to the nonorthogonality term.

The authors would like to thank Professor M. Kawai for valuable discussions and for careful reading of the manuscript. They wish to thank Professor M. Nogami, Professor S. Takagi, and Professor T. Marumori for their encouragement and interest throughout this work. One of the authors (K.-I. K.) acknowledges the support of the Ito Science Foundation. Computer time for using HITAC-8450 was supplied by the College of Science and Technology, Nihon University.

¹C. K. Gelbke *et al.*, Phys. Rev. Lett. **29**, 1683 (1972).

²C. K. Gelbke *et al.*, Phys. Rev. C **9**, 852 (1974).

³R. Vandenbosch *et al.*, Nucl. Phys. **A230**, 59 (1974).

⁴W. von Oertzen, Nucl. Phys. **A148**, 529 (1970); W. von Oertzen and W. Nörenberg, Nucl. Phys. **A207**, 113 (1973).

⁵R. M. DeVries and K.-I. Kubo, Phys. Rev. Lett. **30**, 325 (1973); R. M. DeVries, Phys. Rev. C **8**, 951 (1973).

⁶T. Ohmura, B. Imanishi, M. Ichimura, and M. Kawai, Prog. Theor. Phys. **41**, 391 (1969), and **43**, 347 (1970), and **44**, 1242 (1970); B. Imanishi, M. Ichimura, and M. Kawai, Phys. Lett. **52B**, 267 (1974).

⁷B. Imanishi, in *Proceedings of the Symposium on Cluster Structure of Nuclei and Transfer Reactions Induced by Heavy Ions, Tokyo, Japan, 1975*, edited by H. Kamitsubo, I. Kohno, and T. Marumori (Institute of Chemical and Physical Research, Saitama, Japan, 1975), p. 381.

⁸R. H. Siemssen *et al.*, Phys. Rev. C **5**, 1839 (1972).

⁹P. J. A. Buttle and L. J. B. Goldfarb, Nucl. Phys. **78**, 409 (1966), and **A176**, 299 (1971).

¹⁰S. Kahana, Phys. Rev. C **5**, 2120 (1973).

¹¹K.-I. Kubo, F. Nemoto, and H. Bandō, Nucl. Phys. **A224**, 573 (1974).

¹²K.-I. Kubo, in *Proceedings of the International Conference on Reactions between Complex Nuclei, Nashville, Tennessee, 1974*, edited by R. L. Robinson *et al.*, (North-Holland, Amsterdam, 1974), Vol. I, p. 13.

¹³W. von Oertzen, in *Proceedings of the Symposium on Cluster Structure of Nuclei and Transfer Reactions Induced by Heavy Ions, Tokyo, Japan, 1975*, edited by H. Kamitsubo, I. Kohno, and T. Marumori (Institute of Chemical and Physical Research, Saitama, Japan, 1975), p. 337.

¹⁴C. A. McMahan and W. Tobocman, Nucl. Phys. **A202**, 561 (1973).

Mass Yield Distributions in the Reaction of ^{136}Xe Ions with ^{238}U †

R. J. Otto, M. M. Fowler, D. Lee, and G. T. Seaborg

Lawrence Berkeley Laboratory and Department of Chemistry, University of California, Berkeley, California 94720

(Received 13 October 1975)

Yields of 131 nuclides were measured radiochemically to delineate the mass distribution in the reaction of 1150-MeV ^{136}Xe with a thick ^{238}U target. Six components attributed to either the quasifission or the quasielastic-transfer mechanisms were observed in the mass distribution. An upper limit of 20 mb is given for the fusion-fission process. Neutron-deficient product masses in the region $180 \leq A \leq 210$, colloquially referred to as the "gold finger," are explained as heavy quasifission products.

Attempts to synthesize the "superheavy elements" via the reaction of heavy ions with heavy targets has stimulated considerable interest in the mechanisms of these interactions. The reactions of Kr and Xe ions with uranium are of particular interest because of the possibility of pro-

ducing superheavy elements. The radiochemical mass-yield distribution study for the reaction of 605-MeV ^{84}Kr with ^{238}U by Kratz, Norris, and Seaborg¹ elucidated the complexity of the nuclear reaction mechanisms taking place and the variety of products formed when a fissionable target is

used. Seven components resulting directly or indirectly from three basic reaction mechanisms were identified in their study. The quasielastic transfer mechanisms resulted in two narrow distributions of products, "rabbit ears," peaked at the mass numbers of the target and projectile; in addition, about one-third of the heavy (target) quasielastic transfer products underwent fission, resulting in an asymmetric binary fission distribution. A new reaction mechanism, known by several names such as "deep-inelastic processes,"² "quasifission,"³ "relaxation phenomena,"⁴ and "strongly damped collisions,"⁵ resulted in a "quasi-Kr" product distribution. A symmetric "quasiternary" fission distribution of products attributed to the high-energy binary fission of the complementary heavy "quasi-U" fragments was also seen (we have adopted the "quasi" nomenclature to describe these complementary deep-inelastic components). Based on fission products in the mass region 160 to 180, about 4% of the total reaction cross section was attributed to the fusion-fission mechanism. Neutron-deficient yields near gold with $A \approx 195$, later colloquially referred to as the "gold finger," were not explained at that time.

We have made a similar radiochemical mass-yield study of the reaction of 1150-MeV ^{136}Xe with a thick depleted uranium target. We have measured formation cross sections that represent integrals over the energy and angular distribution of the products and over incident beam energies from the full energy (1150 MeV) down to the reaction barrier. Two depleted uranium targets (30 mg/cm^2) were irradiated with ^{136}Xe ions at 1150 MeV. The first target was bombarded with a total of 2×10^{15} xenon ions and was radiochemically analyzed for "superheavy elements."⁶ The second target, irradiated for 1 h, received a total of 4×10^{14} xenon ions and was used for the mass-yield studies. This target was dissolved and subjected to the same radiochemical group separation scheme⁷ used in the Kr + U experiment.¹ In this case, the superheavy-element fraction and lead fraction were combined. Six chemical fractions were obtained within a few hours after the end of the bombardment. The samples were periodically assayed for γ -ray activities between 40 and 2000 keV over a period of about three weeks. Over 130 nuclides were identified in the six chemical fractions on the basis of γ -ray energy, half-life, and relative abundance. Chemical yield corrections were made for the six chemical groups based on

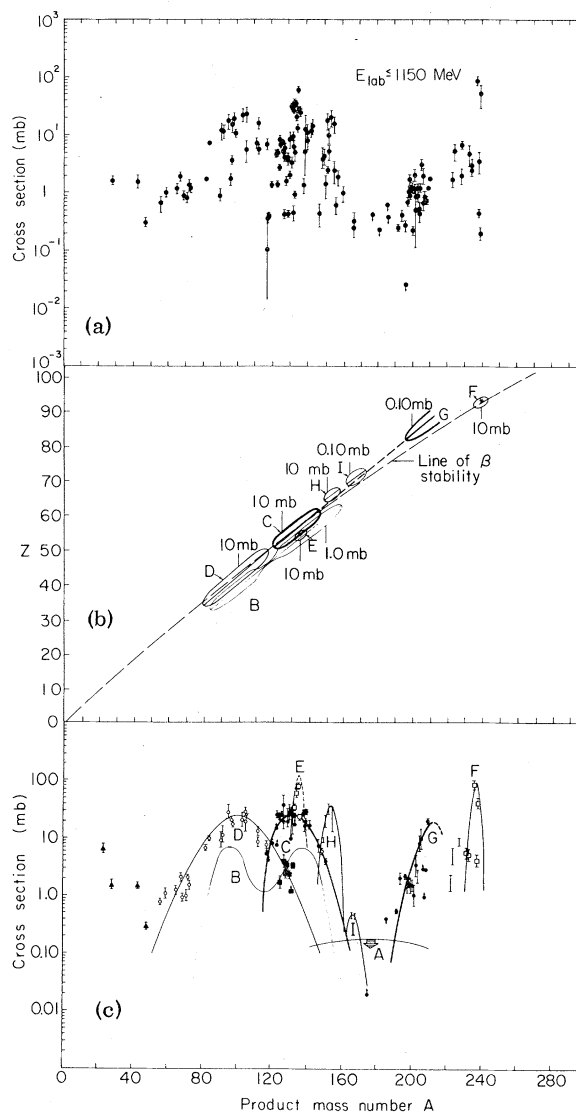


FIG. 1. (a) Independent and cumulative yield formation cross sections for individual isotopes [based on an effective target thickness (17 mg/cm^2 ^{238}U) between incident energy 8.5 MeV/amu and interaction barrier of 5.5 MeV/amu]. (b) Contour lines for equal independent yields in millibarns. (c) Total integrated mass yields. Open circles are chain yields associated with component *D*. Closed circles are chain yields associated with complementary components *C* and *G*. Open squares are chain yields associated with complementary components *E* and *F*, and closed squares with component *B*. Components *H* and *I* were constructed from chain yields ($140 \leq A \leq 180$) shown with error bars only. The data depicted in the region $A \sim 230$ (error bars only) and $A \leq 50$ (solid triangles) are not assigned to any component. Refer to text for explanation of components *A* through *I*.

previous tracer experiments.

Experimentally determined independent and cumulative yields for individual isotopes are

plotted versus mass number in Fig. 1(a). Charge-dispersion descriptions were then determined for small segments of the mass region shown in Fig. 1(a) by applying the following iterative procedure: (1) A charge dispersion description was assumed; (2) independent formation cross sections were calculated for all nuclides in the chosen segment of the mass distribution using the assumed charge-dispersion description along with growth and decay relationships; (3) the independent-formation cross sections were plotted versus $Z - Z_p$, and a new charge dispersion description was obtained (Z_p represents the most probable isobaric charge). The entire procedure was then repeated, often with two overlapping Gaussians having separate Z_p functions. Total chain yields were calculated from the final charge dispersions and the resulting mass-yield distributions were plotted. Figure 1(b) depicts contours in the Z - A plane of constant independent yield and Z_p lines derived from the final charge distributions. The isopleths show the overlap of several mass-yield distributions and their displacement with respect to the line of β stability. Figure 1(c) shows the final chain mass-yield distributions for each of the regions identified in the charge dispersion study.

Component A is shown as an upper limit based on the sensitivity for detection of heavy rare-earth nuclides in the region of $A \approx 180$. This region of A corresponds to prompt symmetric binary fission of the compound nucleus. If we assume a Gaussian shape with a full width at half-maximum of 146 mass units,¹ we calculate an upper limit of 20 mb for the fusion-fission process. Component B is based on the neutron-excessive yields of ^{125}Sn , ^{127}Sn , ^{128}Sn , ^{129}Sb , ^{130}Sb , ^{131m}Te , and ^{132}Te . Based on the $\text{Kr} + \text{U}$ results, a mass distribution corresponding to the fission of ^{238}U with ~ 15 -MeV excitation energy was fitted to these data. Component C was determined from neutron-deficient charge dispersions in the regions $122 \leq A \leq 135$ and $135 \leq A \leq 160$. Component D was obtained by subtraction of the low-energy fission contribution (component B) from the neutron-excessive cumulative yields representing greater than 90% of the chain yields for the composite charge-dispersion description. Cross sections for products near ^{136}Xe that were clearly not on the charge dispersion curve in the $A = 136$ region were attributed to component E . Likewise, cross sections for products near the ^{238}U target were used to define component F . Component G is based on the same neutron-defi-

cient charge-dispersion formula used for component C . Because of the rapidly varying chain yields, the charge dispersion was not well defined in the region $180 \leq A \leq 120$. However, experimentally determined independent yields for ^{194}Au and ^{196}Au , corrected for the slope of the mass distribution in this region, are consistent with the assumed charge dispersion. Finally, components H and I are based on very neutron-deficient yields of light rare-earth isotopes. These two components are the result of reactions of ^{136}Xe respectively with Al and Mg, and with Ar impurities⁸ in the uranium target and its support. A comparison of the integrated cross sections for components A through G is given in Table I.

Many similarities and several important differences are seen when the present $\text{Xe} + \text{U}$ and the $\text{Kr} + \text{U}$ ¹ results are compared. One important difference is that there is no indication in the $\text{Xe} + \text{U}$ mass distribution that the fusion-fission process has occurred. The elastic-transfer mechanism can be assigned to components E and F [Fig. 1(c)]. The asymmetric fission distribution, component B , is the result of low-excitation-energy induced fission of the heavy elastic transfer product near ^{238}U . The reported cross section for $B/2$ (Table I) includes a 15% correction for recoil loss of these fission products. Because of a combination of recoil losses, short half-lives, and stable reaction products, the mass distribution for component E could not be independently determined and therefore was taken to be equal to the cross section of the heavy "rabbit ear" plus half of the asymmetric fission distribution. The mass distribution of the quasi-

TABLE I. Cross section comparison.

Mechanism	Label Figure 1	Cross Section	
		Xe + U	Kr + U [1]
Fusion-fission	A/2	≤ 20 mb	55 ± 15 mb
Quasi-elastic transfer induced fission	B/2	~ 185 mb	200 ± 40 mb
Quasi-fission (light product)	C	600 ± 125 mb	470 ± 70 mb
Quasi-ternary fission	D/2	400 ± 25 mb	420 ± 60 mb
Quasi-elastic transfer (light product)	E	600 mb	700 ± 120 mb
Quasi-elastic transfer (heavy product)	F	~ 415 mb	~ 420 mb
Quasi-fission (heavy product)	G	~ 140 mb	~ 40 mb
Quasi-Fission	$\sigma_{\text{QF}} = C = D/2 + G$	600 ± 125 mb	470 ± 70 mb
Quasi-Elastic Transfer	$\sigma_{\text{ET}} = E = B/2 + F$	~ 600 mb	700 ± 120 mb
Total Reaction	$\sigma_{\text{R}} = A/2 + C + E$	1200 ± 200 mb	1265 ± 205 mb

Xe (deep-inelastic component) formed in the quasifission process is identified as component C [Fig. 1(c)]. This light quasifission-product mass distribution appears to be skewed to the heavy-mass side. About 75% of the complementary quasi-U fragments undergo high-energy binary fission resulting in the broad symmetric fission distribution shown as component D. This process has been referred to as quasiternary fission.¹ Component G, colloquially labeled as the "gold finger" and unexplained in the Kr + U results, can be attributed to the quasifission (deep-inelastic) reaction mechanism. This represents quasi-U products that have survived de-excitation without undergoing fission. The Xe + U "gold finger" is no longer peaked in the gold region but extends up to ²¹⁰At. There is also no indication of a gradual decrease in cross section for heavier masses, possibly because isotopes heavier than $A=210$ typically are short-lived α -particle emitters not detected in this work. Formation cross sections for ²²⁴Ra, ²²⁸Ac, and ²²⁸Th are plotted in this region.

The above interpretation is supported by a mass balance of the composite mass distribution. Complementary masses and charges in the quasi-Xe and quasi-U distributions (components C and G) plus 20 neutrons derived from the final Z_p functions account for all of the mass and charge of the composite system ($A=374$, $Z=146$). Although the charge of complementary quasifission products indicate that no charged particles were evaporated, we find that the unchanged charge-distribution Z_p formalism which we used is not very sensitive to the detection of the possible evaporation of charged particles with $N/Z \approx 1$, such as α particles or ¹²C particles. The sum of one half of the quasiternary fission cross section ($D/2$) and the cross section for quasi-U products (G) is 540 mb. This, within error limits, is equal to the 600-mb cross section for the quasi-Xe products (component C), as it should be according to our interpretation. In addition, we have made a radiochemical mass-yield study of the reaction of 730-MeV Kr with a thick bismuth target. The quasi-Bi mass distribution shows the same trend seen as component G in Fig. 1(c) with the exception that it extends up into the bismuth region. In Table I we see that a larger frac-

tion of the total reaction cross section for Xe + U than for Kr + U has gone into quasifission. The total reaction cross section is given by the sum of the components A/2, C, and E, and is thus experimentally determined to be 1200 ± 200 mb. This appears to be a reasonable value for the mean cross section for reactions occurring over the energy range from the interaction barrier, about 750 MeV, and the full energy of the incident ¹³⁶Xe beam, 1150 MeV (where a reaction cross section of about 2500 mb is calculated). If 15.0 fm is taken as the grazing distance, then the Coulomb barrier for ¹³⁶Xe on ²³⁸U is 750 MeV in the lab system. The mean geometrical cross section is estimated from these values as

$$\bar{\sigma}_r = \pi R^2 \int_B^E \frac{(1 - B/E) dE}{E - B} = 1400 \text{ mb,}$$

where $B=750$ MeV, $R=15.0$ fm, and $E=1150$ MeV. This is in agreement with the experimental value.

We especially thank Dr. A. Ghiorso for his continued advice, guidance, and support. We also wish to thank Mr. Irwin Binder for his assistance. We thank Dr. E. K. Hulet (Lawrence Livermore Laboratory) for the Al-backed U targets.

†Work supported by the U. S. Energy Research and Development Administration.

¹J. V. Kratz, A. E. Norris, and G. T. Seaborg, Phys. Rev. Lett. **33**, 502 (1974).

²A. G. Arkuth, G. F. Gridnev, V. L. Mikheev, V. V. Volkov, and J. Wilczynski, Nucl. Phys. **A215**, 91 (1973).

³F. Hanappe, M. Lefort, C. Ngø, J. Péter, and T. Tamain, Phys. Rev. Lett. **32**, 738 (1974); J. Péter, C. Ngø, and V. Tamain, J. Phys. (Paris), Lett. **36**, L23 (1975).

⁴J. Galin, L. G. Moretto, R. Babinet, R. Schmitt, R. Jared, and S. G. Thompson, Lawrence Berkeley Laboratory Report No. LBL-4064 (to be published).

⁵K. L. Wolf, J. P. Unik, J. R. Huizenga, J. Birkelund, H. Freiesleben, and V. E. Viola, Phys. Rev. Lett. **33**, 1105 (1974); J. P. Bondorf, J. R. Huizenga, M. I. Sobel, and D. Sperber, Phys. Rev. C **11**, 1265 (1975).

⁶G. T. Seaborg, M. M. Fowler, and R. J. Otto, to be published.

⁷J. V. Kratz, J. O. Liljenzin, and G. T. Seaborg, Inorg. Nucl. Chem. Lett. **10**, 951 (1974).

⁸The target was made by sputtering U in an Ar atmosphere. A 1/20 atom ratio ⁴⁰Ar/²³⁸U was determined by charged-particle activation analysis.